ORIGINAL ARTICLE

Bright spectroscopic binaries: I. Orbital parameters of five systems with periods of $P < 365$ days

Dennis Jack[1] | **Missael Alejandro Hernández Huerta[1]** | **Klaus-Peter Schröder[1,2]**

[1]Departamento de Astronomía, Universidad de Guanajuato, Guanajuato, Mexico

[2]Sterrewacht Leiden, Universiteit Leiden, Leiden, The Netherlands

Correspondence

Dennis Jack, Departamento de Astronomía, Universidad de Guanajuato, A.P. 144, 36000 Guanajuato, GTO, Mexico.
Email: dennis.jack@ugto.mx

Funding information

Universidad de Guanajuato

Abstract

In a well-aimed search based on the recently published Gaia DR2 radial velocity data and performed with the robotic TIGRE telescope, we have discovered 19 bright ($m_V < 7.66$ mag) spectroscopic binary stars. We present the radial velocity curves of five of these stars (HD 20656, HD 27259, HD 98812, HD 150600, HD 193082) with periods of $P < 365$ days. We determined their orbital parameters using the toolkit RadVel. The complete set of basic stellar parameters (effective temperature, surface gravity, metallicity, mass, and age) of the primary stars are determined using the observed intermediate resolution spectra ($R \approx 20,000$) with iSpec and a comparison of the position in the Hertzsprung-Russell diagram with stellar evolution tracks. All five primary stars have already evolved to the giant phase and possess low-mass secondaries, which do not noticeably affect the spectra. Finally, we determined the minimum masses of the secondary stars of the binary systems and present conclusions about the properties of the binary systems.

KEYWORD

binaries: spectroscopic – techniques: radial velocities – stars: fundamental parameters – stars: individual (HD 20656, HD 27259, HD 98812, HD 150600, HD 193082)

1 | INTRODUCTION

Many of the stars in our Galaxy are found to be part of binary or multiple stellar systems because this is a natural outcome of the star formation process (Duchêne & Kraus 2013). The total binary fraction in the solar neighborhood is about 50% (Raghavan et al. 2010). Studying these multiple star systems allows us to directly determine the masses of the binary components giving us a better insight into the understanding of stellar population and evolution. Close and interacting binaries may even alter the evolution of the companion star making it definitely worth finding and studying binary and multiple stellar systems in detail.

There exist different detection methods for the discovery of binary systems, which led to the publication of several catalogs of the different types of binary stars. For example, a catalog of visual binary stars has been published in The Washington Double Star Catalog (Mason et al. 2018). The methods for the detection of binary stars are the same as for discovering exoplanets. Thus, many exoplanet detection programs have also discovered more and more binary star systems. One important example is the Kepler mission (Borucki et al. 2010), which used photometric observations to detect eclipses of stars by their companions or exoplanets (transits). This mission resulted in a very large catalog of eclipsing binary stars (Kirk et al. 2016).

Detecting periodic variations in the radial velocity by performing spectroscopic analyses of stars is another successful method for the discovery of binary systems and exoplanets. There are a few catalogs of spectroscopic binary systems and their orbital parameters like the 9th Catalog of Spectroscopic Binary Orbits (Pourbaix et al. 2004) or the CHARA Catalog of Spectroscopic Binary Stars (Taylor et al. 2003). Detecting and studying spectroscopic binary systems requires intermediate to high spectral resolution, while the signal-to-noise ratio can still be relatively low. A wide spectral range also helps to determine the radial velocity more precisely. Several observations have to be performed at different epochs in order to clearly unveil radial velocity changes and thus, the binarity of the star system. Obtaining a complete radial velocity curve, at best covering several orbits, allows one to determine the orbital parameters of the respective binary star and to make conclusions about the invisible secondary star.

The ESA Gaia mission (Gaia Collaboration et al. 2016) published its second Data Release (DR2) (Gaia Collaboration et al. 2018) in March 2018. Measurements of the radial velocity of about 7.2 million stars are included in DR2 (Katz et al. 2019). However, the published values are only mean values of several measurements of the radial velocity. Large "errors" in the Gaia DR2 radial velocities can have several causes. One important possibility is that the large scatter may indicate binarity of the observed star. Therefore, observing these stars with large radial velocity scatter in a follow-up observation program will lead to the discovery of new spectroscopic binary systems. Obtaining detailed radial velocity curves in these follow-up programs will also permit a determination of the orbital parameters in order to obtain some information about the invisible secondary star.

We present the results of the study of five bright spectroscopic binaries. We describe the selection of our observational sample in Section 2. The determination of the orbital parameters is presented in Section 3. Section 4 contains the results of the determination of the stellar parameters using spectral analysis and comparison with stellar evolution tracks. After a discussion of the detailed results of each star in Section 5, we present our conclusions in Section 6.

2 | OBSERVATIONAL STRATEGY

We describe the selection of our observational sample of stars for which we obtained time series of spectra determining the respective radial velocities (RV).

2.1 | Selection of the candidate stars

We selected a sample of candidate stars that we expected had a high probability to be spectroscopic binaries. To obtain this sample, we made use of the archive of Gaia DR2. We searched for stars that show large scatter of the RV measurement and are easily observable with the TIGRE telescope in Central Mexico. As a criterion for the minimal error size in the Gaia DR2 measurements of the RV, we selected stars with a scatter of > 2 km s^{-1}. We selected only stars that rise at least 70° above the horizon at the location of the telescope (latitude of +21°) to guarantee good observability of the candidate star over a long period. In order to select only bright stars, we set the required G-band brightness of the Gaia DR2 observations to be brighter than 7.0 mag. An additional criterion was that all-stars need to have a determined Gaia DR2 parallax to be able to locate the stars in the Hertzsprung-Russell diagram (HRD) and thus, determine their masses and ages. In the last selection step, we discarded all-stars that were already identified as binary or variable stars, or already have precise radial velocity measurements listed in SIM-BAD. The final sample of stars that are candidates for being spectroscopic binary stars consisted of 19 stars.

2.2 | Radial velocity measurements

The observations of our sample of 19 stars were performed with the 1.2 m robotic telescope TIGRE, which is located at the Observatory La Luz close to the town of Guanajuato in Central Mexico. We obtained intermediate resolution spectra ($R \approx 20,000$) using the HEROS echelle spectrograph. The spectrograph covers the whole optical wavelength range in two arms from 3,800 to 8,800 Å, having a small gap of about 100 Å between the two channels (red and blue) around 5,800 Å. The observations are performed automatically without any human interaction making it an ideal telescope for monitoring of stars. For a more detailed description of the technical components and the automatic reduction pipeline consult Schmitt et al. (2014).

For all TIGRE observations, the RVs are determined automatically during the reduction process of the data. The method is explained in detail in Mittag et al. (2018), where the RV curve of a spectroscopic binary was analyzed. As a first step telluric lines are used to better calibrate the wavelength solution. This can only be done in the red channel since the blue channel does not contain any telluric lines. The RV is then determined by applying a cross-correlation with a reference spectrum taken from a set of synthetic spectra using PHOENIX models (Husser et al. 2013). The mean precision of this automatic

TABLE 1 The orbital parameters of the five spectroscopic binary systems determined by an analysis of the radial velocity curve using RadVel

Star	P (days)	T_c (JD)	e	K (km s^{-1})	ω (rad)	v_{rad} (km s^{-1})
HD 20656	159.577 ± 0.043	8496.608 ± 0.091	0.2298 ± 0.0016	24.211 ± 0.043	0.5381 ± 0.0078	18.671 ± 0.028
HD 27259	188.11 ± 0.23	8411.9 ± 0.63	0.0203 ± 0.0066	9.97 ± 0.057	0.44 ± 0.38	3.401 ± 0.044
HD 98812	137.33 ± 0.12	8373.67 ± 0.28	0.0051 ± 0.0045	9.558 ± 0.048	—	-32.107 ± 0.036
HD 150600	123.195 ± 0.039	8300.136 ± 0.088	0.5995 ± 0.0043	13.166 ± 0.092	1.331 ± 0.012	-7.448 ± 0.041
HD 193082	50.395 ± 0.014	8281.23 ± 0.14	0.0038 ± 0.0036	9.896 ± 0.054	—	-89.683 ± 0.039

RV determination is about 0.11 km s^{-1} (Mittag et al. 2018). This is a mean value for good observational conditions. The individual errors of our RV measurements can be found in the electronically available data.

Since all-stars of the sample are bright (6.54 mag $\leq m_V \leq$ 7.66 mag) and we do not require spectra with a very high signal-to-noise ratio we opted for an exposure time of just 1 min per observation. For our observational campaign, we took three spectra of each star in the sample, distributed over a longer period in order to detect variations in the RV. In the case of a positive detection, we obtained a longer time series of spectra to obtain the respective radial velocity curves for an analysis of the binary systems.

3 | BINARY ORBITS

We found that all 19 observed candidate stars in our sample were spectroscopic binary stars. Among these, we found five spectroscopic binaries (HD 20656, HD 27259, HD 98812, HD 150600, and HD 193082) with periods shorter than 1 year. We determined the orbital parameters by analyzing the measured radial velocity curves. All individual RV measurements from the TIGRE observations are electronically available (http://www.astro.ugto.mx/~dennis/binaries/).

3.1 | RadVel

We used the Radial Velocity Modeling Toolkit RadVel (Fulton et al. 2018) (version 1.3.1) to analyze the RV curves and to determine the orbital parameters. Although developed for the analysis of RV curves for the study of exoplanets, it works very well for binary stars, since the underlying physical problem is the same. In RadVel, the RV curves are fit by using six independent parameters the orbital period P, the time of inferior conjunction T_c, eccentricity e, semi-amplitude K, the argument of the periapsis of the star's orbit ω, and the RV of the system v_{rad}. After giving the initial guesses of the six orbital parameters, the set of equations for the Keplerian orbit is solved by an iterative method in order to determine the best fit for the observed RV curve.

We first created a generalized Lomb-Scargle periodogram to check for possible periods in the RV measurements. All-stars show a strong peak around the determined orbital periods. We then applied the above-described procedure for the determination of the orbital parameters with RadVel. To obtain an estimation of the uncertainties we used the Markov-Chain Monte Carlo (MCMC) package of Foreman-Mackey et al. (2013) included in RadVel.

3.2 | Orbital parameters

In Table 1, we present the results of the orbital parameter fitting procedure, including the errors that we obtained from the MCMC run. The stars HD 27259, HD 98812, and HD 193082 have close to circular orbits so that a determination of the parameter ω is not possible within the errors of the MCMC run. The star with the largest semi-amplitude is HD 20656, while the rest of the stars show a similar semi-amplitude K of around 10 km s^{-1}. The star HD 150600 with $e = 0.5995$, has a quite eccentric orbit.

In Figure 1 we show the observed radial velocity curve of HD 20656 including the RadVel fit curve. In subplot (a) we show the complete observations of more than 1 year of radial velocity measurements (circles), including the fit of RadVel (solid line) covering more than two orbital periods. Subplot (b) presents the residuals showing that we obtained a very good fit within the errors of the RV measurements. The phase-folded plot of the radial velocity curve is presented in subplot (c). The orbit has a moderate eccentricity $e = 0.2298$.

The radial velocity curve of HD 27259 and the respective RadVel fit is shown in Figure 2. This star has the longest period of the five stars of our sample. In fact, we hardly covered two orbital periods during our observation campaign. In Figure 3, we present the complete RV
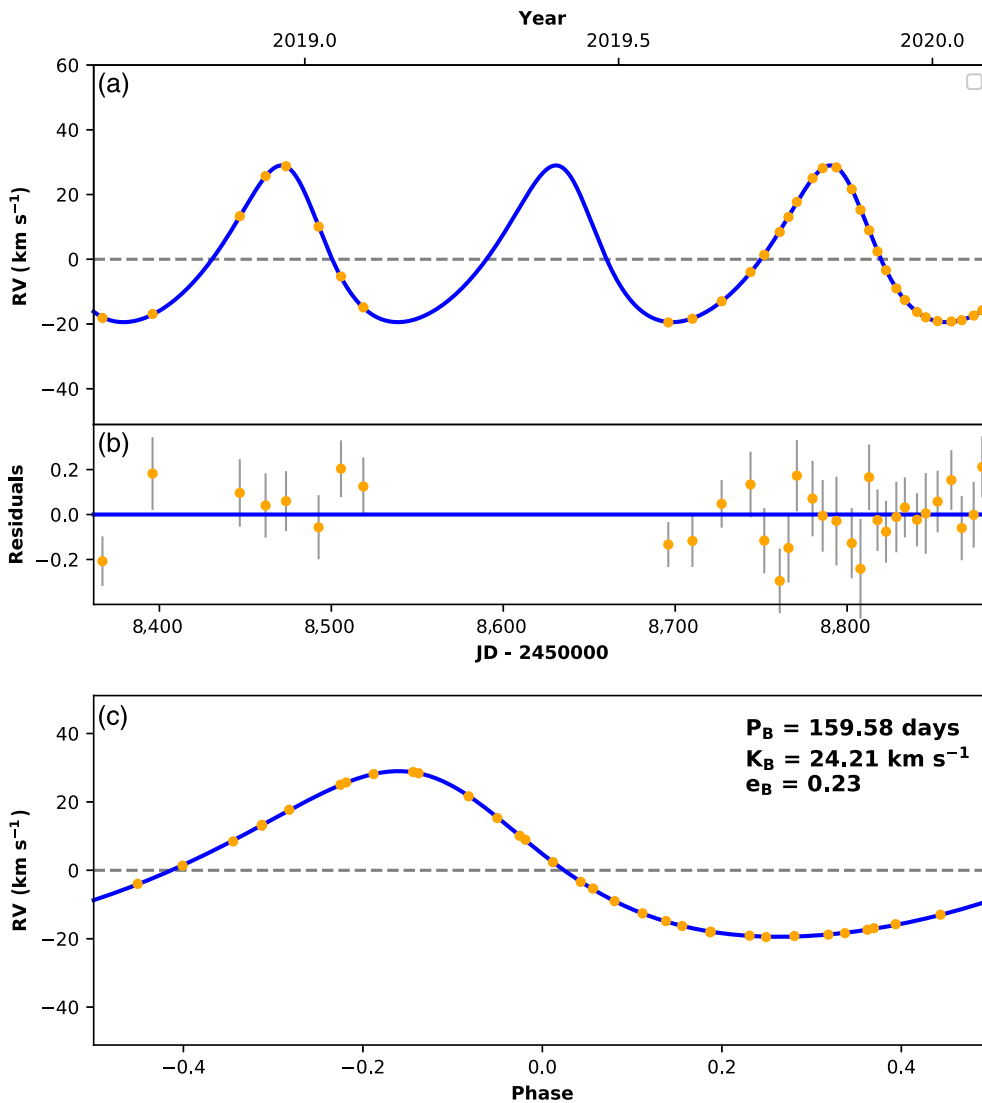
FIGURE 1 Radial velocity curve of HD 20656: (a) the complete measurements (circles) and RadVel fit (solid line), (b) the residuals, and (c) the phase-folded RV curve

measurements of the star HD 98812, including the RadVel fit. We covered almost three complete orbital periods of the RV curve. The radial velocity curves, observations, and the RadVel fit, of HD 150600 are displayed in Figure 4. We covered more than four orbits during our observational campaign. This star has the most eccentric orbit with a value of $e = 0.5995$ showing a very steep decrease of the radial velocity. The last star in our sample, HD 193082, has the shortest orbital period, and the RV curve fit is presented in Figure 5. We were able to cover more than ten orbits. The well-covered RV curve of HD 193082 demonstrates that this star has a circular orbit.

4 | STELLAR PARAMETERS OF THE PRIMARY STARS

To be able to fully study the binary systems, including the invisible companion star, we determined all stellar parameters of the primary stars analyzing the intermediate resolution spectra obtained with the TIGRE telescope. By locating the stars in the HRD and using stellar evolution tracks, we were also able to determine the masses and ages of the systems.

4.1 | Distances and luminosities

In Table 2, we list the observational properties of the five spectroscopic binary stars, spectral type, and apparent magnitude in the V-band (m_V) as given in the SIMBAD database. The parallaxes in milliarcseconds (and distances in parsecs) were taken from the Gaia DR2 archive. Due to the movement of the primary star on its binary orbit, it will also have a projected movement on the sky. This may alter the detected annual movement caused by the parallax. The size of this effect depends on several circumstances. The orbital period P is important, but for short
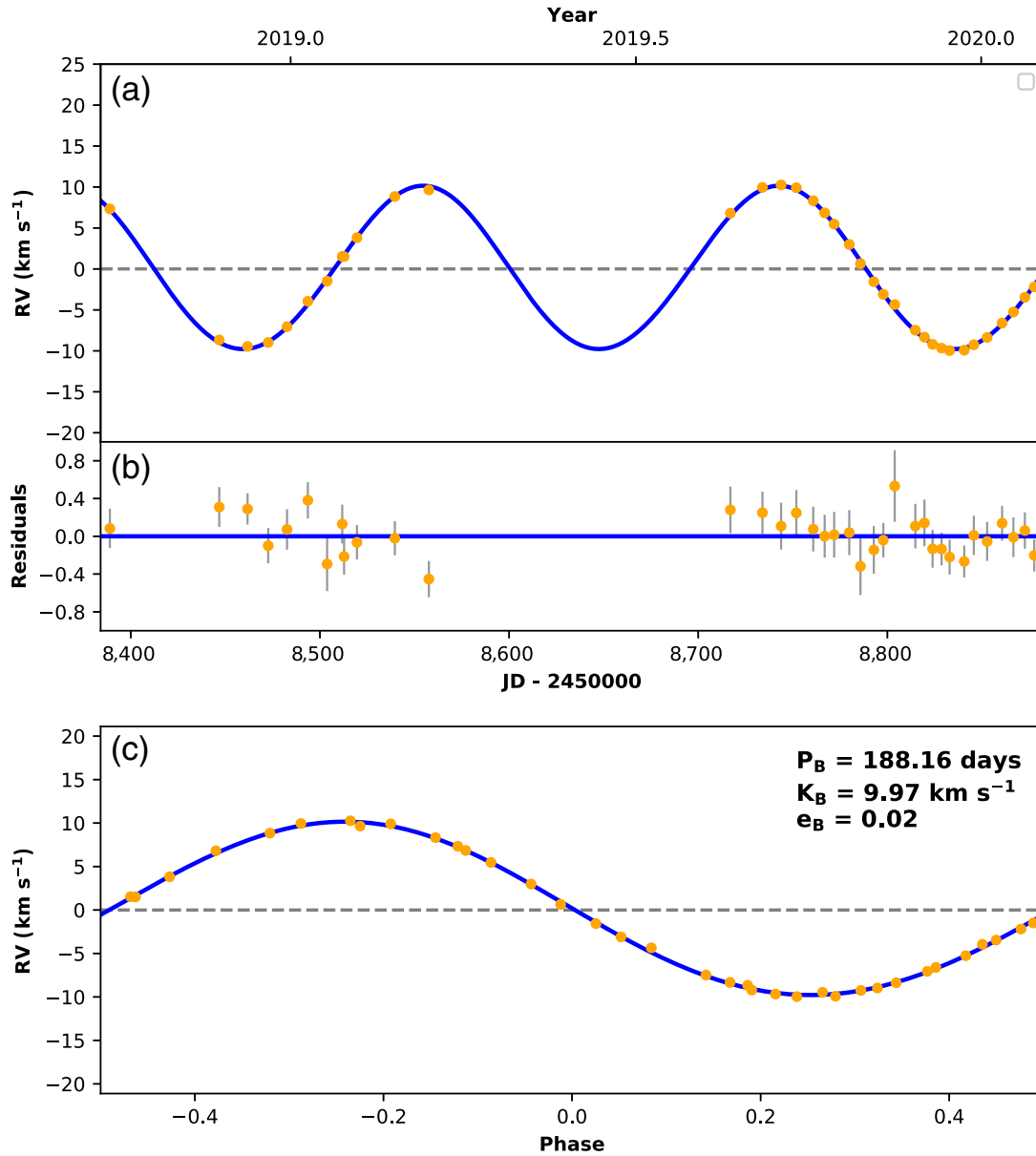
FIGURE 2 Radial velocity curve of HD 27259: (a) the complete measurements (circles) and RadVel fit (solid line), (b) the residuals, and (c) the phase-folded RV curve

periods ($P \ll 1$ year) the effect will be averaged out. For periods around 1 year, the effect will be the largest. However, the final effect on the parallax measurement depends strongly on the orientation of the binary orbit. If the movement of the primary star on its orbit is perpendicular to the movement due to the parallax there is no net effect. The effect is strongest when parallax and orbital movement are aligned. This makes it hard to estimate an error since the orientation is intrinsically unknown. However, one should keep in mind a possible large systematic effect on the Gaia DR 2 parallaxes of binaries. In the following, we give estimates of this effect for our stars based on our analysis. The Gaia DR2 distances were used to determine

the absolute magnitudes in the V-band (M_V). Using the bolometric corrections (BC) of Flower (1996), we obtained the absolute bolometric magnitude M_{bol}. We calculated the luminosity L (in solar luminosities $L_\odot$) of the five stars, and present the result in the last column of Table 2.

4.2 | Spectral analysis

For the measurements of RV, we obtained intermediate resolution spectra with a relatively low signal-to-noise ratio (S/N). In the red channel the mean S/N is about 30 for each spectrum while in the blue channel, depending on the spectral type, the S/N lies somewhere in the range
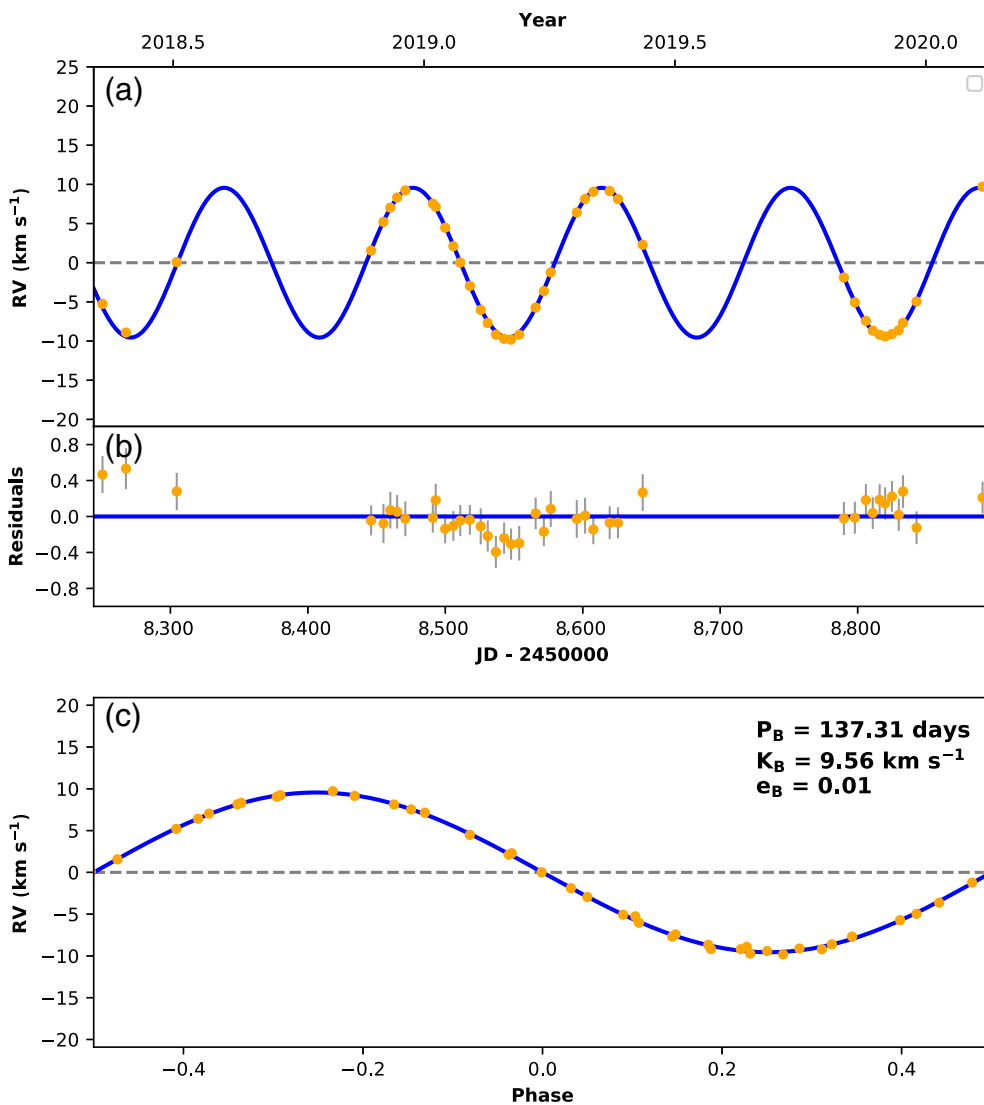
FIGURE 3 Radial velocity curve of HD 98812: (a) the complete measurements (circles) and RadVel fit (solid line), (b) the residuals, and (c) the phase-folded RV curve

In panel (c):
$P_B = 137.31$ days
$K_B = 9.56$ km s^{-1}
$e_B = 0.01$

TABLE 2 Observational properties of five spectroscopic binary stars with periods of less than 1 year. The luminosities L were determined from the distances and bolometric corrections (BC)

Star	Spec. type	m_V	parallax (mas)	distance (pc)	M_V	BC	M_{bol}	L ($L_\odot$)
HD 20656	F8	7.14 ± 0.01	3.98 ± 0.05	251.3 ± 3.1	0.14 ± 0.03	-0.176 ± 0.016	-0.03 ± 0.03	86 ± 3
HD 27259	K5III	7.66 ± 0.01	3.74 ± 0.07	267.4 ± 5.1	0.52 ± 0.04	-0.848 ± 0.053	-0.33 ± 0.07	113 ± 7
HD 98812	K0	7.43 ± 0.01	2.15 ± 0.07	466 ± 16	-0.91 ± 0.08	-0.865 ± 0.036	-1.78 ± 0.09	427 ± 36
HD 150600	K0	7.19 ± 0.01	8.15 ± 0.16	122.6 ± 2.4	1.75 ± 0.04	-0.342 ± 0.020	1.40 ± 0.04	23 ± 1
HD 193082	G8IV	7.37 ± 0.01	3.58 ± 0.05	279.4 ± 3.7	0.14 ± 0.03	-0.601 ± 0.025	-0.46 ± 0.04	127 ± 5

5–10. In order to obtain one spectrum with a high S/N, we combined 15 spectra of each star using the spectra with the highest S/N. Each individual spectrum was corrected for the measured RV, which is determined only in the red channel. Therefore, we corrected the respective blue spectra for the same RV as measured in the red channel, because the S/N in the blue channel is too low to determine the radial velocity.

For the determination of the stellar parameters, we used the spectral analysis toolkit iSpec (Blanco-Cuaresma et al. 2014). The latest version (v2019.03.02) (Blanco-Cuaresma 2019) allows for a comparison of observed spectra with synthetic spectra determining the selected free parameters by a χ^2 method. Several different atmospheric models, radiative transfer codes, references for the solar abundances, and line
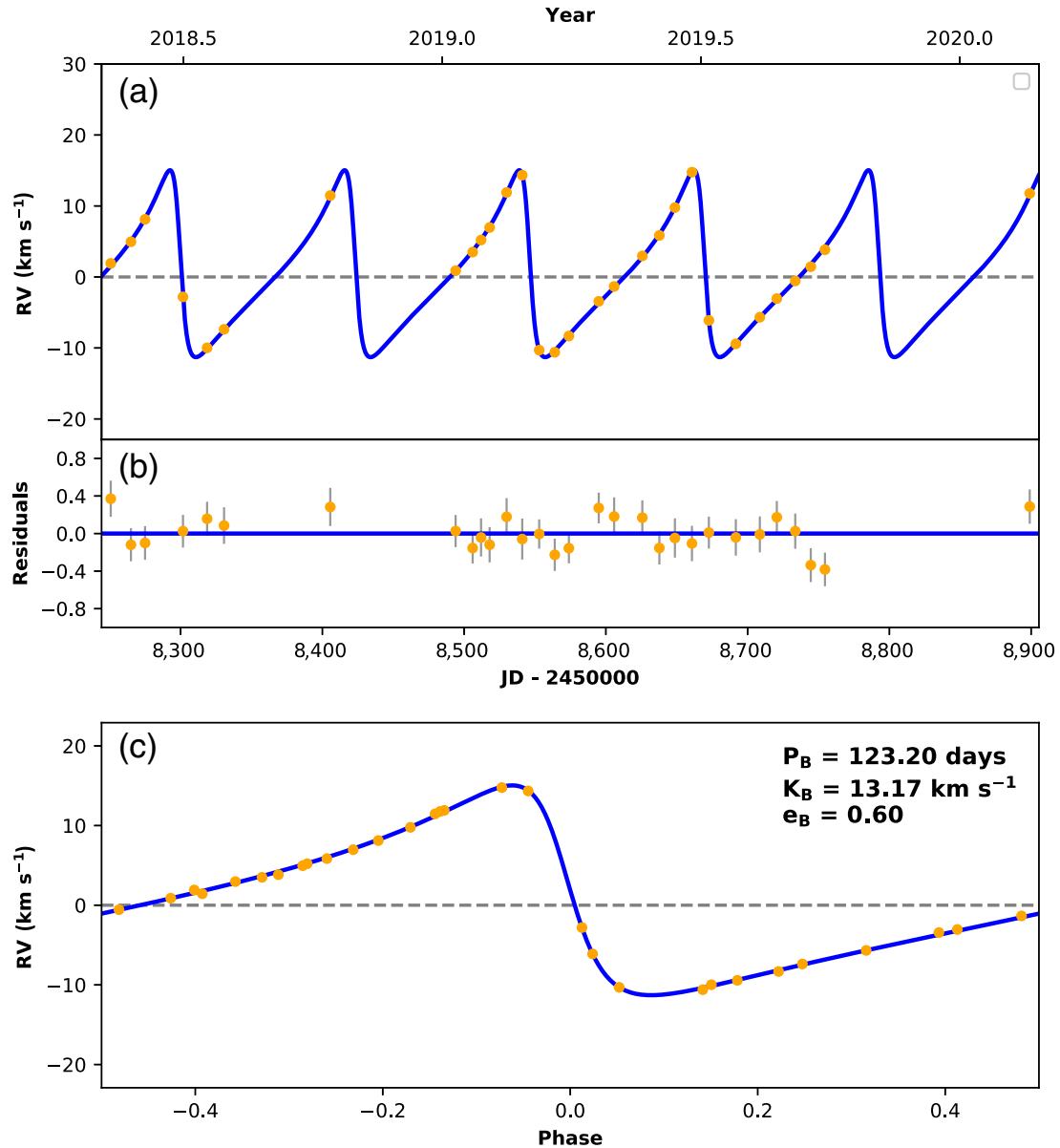
FIGURE 4 Radial velocity curve of HD 150600: (a) the complete measurements (circles) and RadVel fit (solid line), (b) the residuals, and (c) the phase-folded RV curve

lists can be chosen during the analysis. We used the grid of MARCS atmosphere models (Gustafsson et al. 2008) included in iSpec. For the reference solar abundances, we used the values published in Grevesse et al. (2007), which are also implemented in iSpec. The synthetic spectra were calculated using the radiative transfer code SPECTRUM (Gray & Corbally 1994). The list of atomic lines that were used for the spectrum calculation was taken from the Gaia-ESO Survey line-list (Gilmore et al. 2012; Randich, Gilmore,, & Gaia-ESO Consortium 2013). All these are the recommended options for spectral analysis with synthetic spectra with iSpec (Blanco-Cuaresma 2019).

For the analysis of our observed spectra in iSpec, we selected several segments between wavelengths of 4,900

and 8,800 Å excluding regions with known strong telluric contamination. For our analysis, we did not use the proposed procedure of using the list of selected lines (Blanco-Cuaresma 2019) that obtain a good fit for the solar spectrum, since we found a strong dependence of the final fits for our stars on the selected initial values (Schröder et al. 2020b).

As free parameters for the fitting procedure, we selected the effective temperature T_{eff}, the surface gravity $\log g$, the metallicity $[M/H]$ of the star, and the recently added parameter of the alpha enhancement $[\alpha/Fe]$. The micro and macro turbulence velocities (v_{mic}, v_{mac}) were determined with the empirical relations included in iSpec in order to be able to determine the rotational velocity
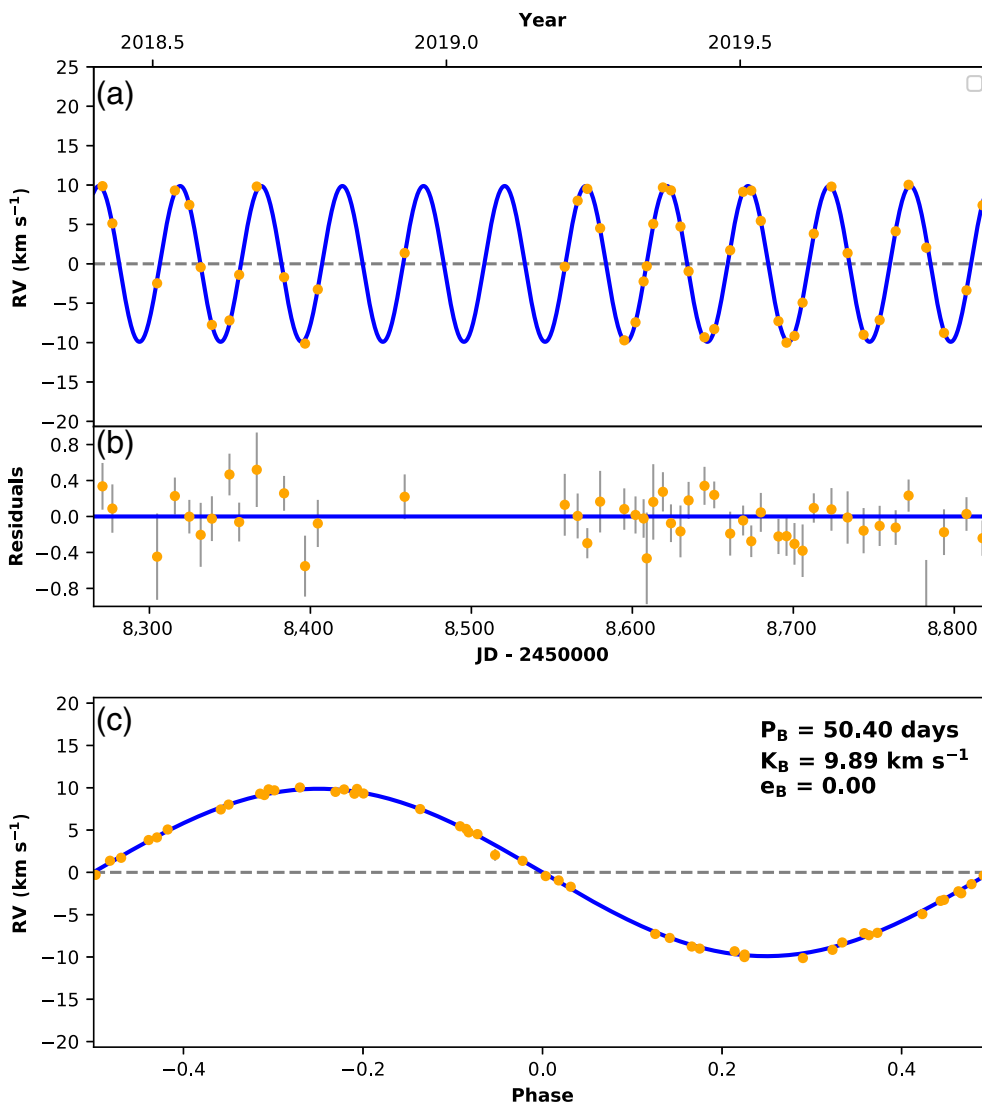
FIGURE 5 Radial velocity curve of HD 193082: (a) the complete measurements (circles) and RadVel fit (solid line), (b) the residuals, and (c) the phase-folded RV curve

$v \sin i$ more precisely, where i stands for the inclination of the rotational axis of the star. However, the determination of $v \sin i$ may still not be very accurate. It is difficult to determine the rotational velocity with iSpec since it is determined from the line profiles, which are also affected by the micro and macro turbulence velocities. The systematic uncertainties of such an analysis with iSpec or other synthesizing tools, especially on intermediate resolution spectra like the ones we employ here, have been studied by us in detail in a separate publication (Schröder et al. 2020a). The main concern is cross-talk between one badly set parameter and its effects on the selection of the others since the still relatively broad instrumental spectral profile dilutes any parameter-specific information in the line profile. Nevertheless, we found that by following a consistent procedure and making use of non-spectroscopic information, TIGRE/HEROS spectra can be interpreted to within reasonable variances of, for example, for the effective temperature of about 70 K, when compared with

higher spectral resolution results (e.g., PASTEL database), and even the rotation velocities obtained by iSpec on TIGRE spectra have a residual variance of only 2.5 km s^{-1}. While the slightly higher iSpec-own choice of the preset turbulence velocities, as used here, may be compensated for by somewhat smaller rotation velocity solutions, this does not exceed underestimates of about 2 km s^{-1}.

The results of the described spectral analysis with iSpec are presented in Table 3, where the given errors are pure fitting errors and do not include any systematic errors mentioned above. The effective temperatures for the sample range from about 4,200 to 5,350 K, indicating that the stars are of G or K spectral type. The values for the surface gravity clearly show that all stars are actually giant stars, as was also obtained from the absolute magnitudes in the V-band calculated using the parallaxes (Table 2). However, it is difficult to obtain exact values for log(g) using spectroscopy. A reasonable error for the surface gravity determined with iSpec can be up to ±0.5 (Schröder

TABLE 3 Basic stellar parameters of the five spectroscopic binaries determined with spectral analysis using iSpec

Star	T_{eff} (K)	$\log g$	[M/H]	[α/Fe]	v_{mic} (km s^{-1})	v_{mac} (km s^{-1})	$v \sin i$ (km s^{-1})
HD 20656	5357.9 ± 10.7	2.79 ± 0.03	0.04 ± 0.01	0.00 ± 0.01	1.36	3.94	10.55 ± 0.14
HD 27259	4211.2 ± 5.2	1.47 ± 0.02	0.17 ± 0.01	0.04 ± 0.01	1.58	4.45	11.3 ± 0.1
HD 98812	4197.0 ± 6.7	0.98 ± 0.02	-0.24 ± 0.01	0.07 ± 0.01	1.62	5.36	5.93 ± 0.11
HD 150600	4915.7 ± 9.4	2.98 ± 0.02	0.09 ± 0.01	0.01 ± 0.01	1.26	3.69	6.92 ± 0.11
HD 193082	4506.1 ± 9.3	2.49 ± 0.02	-0.32 ± 0.01	0.17 ± 0.01	1.34	4.30	17.7 ± 0.1

et al. 2020b). All five stars have reasonable values for the metallicity and alpha enhancement. HD 193082 has with a value of $v \sin i = 17.7$ km s^{-1} a quite high rotational velocity for a giant star. Actually, all-stars show a high rotational velocity for being giant stars. As mentioned above, determining low values for $v \sin i$ is a difficult task in iSpec. Since we observe RV variations for these stars they have probably an inclination of close to $i = 90°$, which could contribute to the high rotational velocities. Of course, we assume that the inclination of the rotational axis of the primary stars and of the orbits around the companion stars are similar.

4.3 | Ages and masses

Having the luminosities and effective temperatures of the primary stars we can now place them in the HRD. We then used stellar evolution tracks that we computed with the Cambridge (United Kingdom) Eggleton code in its updated version (Pols et al. 1997; Pols et al. 1998) assuming solar metallicity ($Z = 0.02$) to fit these evolution tracks to the position of the stars in order to determine the ages and masses of the five spectroscopic binary stars of our sample. The results are presented in Table 4. The errors in the ages are relatively large. In Figure 6, we show the positions of the five spectroscopic binary stars in the theoretical HRD. The solid lines show the stellar evolution tracks with the best fit mass for each star. All five stars are evolved, have left the main sequence, and are found to be in their giant phase. The positions in the HRD are also consistent with the determination of the surface gravity log(g) given in Table 3. The star HD 98812 has also the lowest value for the surface gravity, the star at the upper right, the most evolved of the sample.

5 | DISCUSSION OF THE RESULTS

Thanks to a complete analysis of the RV curves of the stars to obtain the orbital parameters as well as to the analysis of the intermediate resolution stellar spectra and the

TABLE 4 The masses and ages of the five primary stars of the spectroscopic binaries determined with fitting stellar evolution tracks to the positions in the Hertzsprung-Russell diagram

Star	Mass [$M_\odot$]	Age (Myr)
HD 20656	2.73 ± 0.08	509 ± 38
HD 27259	1.05 ± 0.15	12530 ± 6200
HD 98812	2.15 ± 0.20	1157 ± 180
HD 150600	1.70 ± 0.20	2142 ± 735
HD 193082	1.88 ± 0.28	1700 ± 710

comparison with stellar evolution tracks that gave us all the basic stellar parameters of the primary stars, we are now able to determine some parameters of the companion star of each binary system.

5.1 | Determination of the secondary mass

Using Kepler's laws one can derive a formula that connects the masses of the two components of a binary system with three observable orbital parameters, which are the orbital period P_{orb}, semi-amplitude K, and the eccentricity e. This so-called mass function f is calculated by the formula

$$f = \frac{M_2^3 \sin^3 i}{(M_1 + M_2)^2} = \frac{P_{\mathrm{orb}} K^3}{2\pi G}(1 - e^2)^{3/2},$$

where G represents the gravitational constant. Since we determined the masses of the primary stars (M_1), we can calculate the minimal masses of the secondary stars ($M_2 \sin i$). We revised the observed spectra, which have an S/N of about 50, and did not find any indication of spectral lines of the secondary. Thus, the apparent non-visibility of the companion flux in the spectrum should set an upper limit of L_1:L_2 of 50:1, which would via $L \propto M^4$ give an upper limit of the secondary mass M_2 as $M_1/2.6$ since $2.6^4 \approx 50$, which is consistent with the minimal masses in Table 5. In
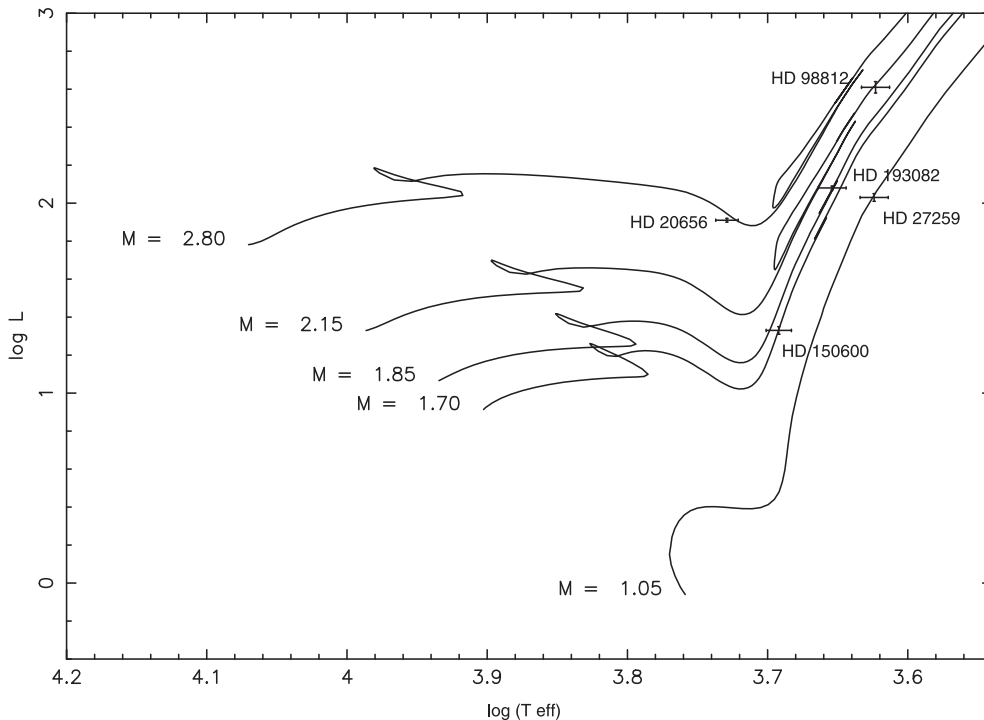
FIGURE 6 Positions of the five stars in the Hertzsprung-Russell diagram and the best fitting stellar evolution tracks (solid lines) of the respective masses. All stars are in the giant phase

the following, we will discuss the individual conclusions that can be derived from our detailed analysis of all five binary systems.

5.2 | HD 20656

The primary star has a mass of $2.7\,M_\odot$ and has left already the main sequence ($\log g = 2.8$) giving it a stellar classification as a G type giant star with an effective temperature of about 5,360 K. In fact, the determined stellar parameters contradict the SIMBAD suggested a spectral type of F8. The metallicity is close to the solar one ($[M/H] = 0.04$). This star at 510 Myr is the youngest of the sample.

The eccentric orbit ($e = 0.23$) shows a relatively high amplitude of $K = 24.2$ km s^{-1}. The period is about 159.6 days. Using these orbital parameters, we determined for the minimal mass of the companion star a value of $M_2 \sin i = 1.25 M_\odot$. Thus, the companion definitely has a higher mass than the Sun and is probably an F type star still on the main sequence due to the young age of the system. The high rotational velocity indicates that the system probably has an inclination of close to $i = 90°$.

5.3 | HD 27259

The star HD 27259 has a close to a circular orbit with a period of about half a year ($P = 188.1$ days). The mass is close to solar ($M_1 = 1.05 M_\odot$), which makes it difficult to

determine the exact age of the system. Since the primary star has already evolved from the main sequence the age must be quite large. The primary star has a low temperature of 4,210 K, a low surface gravity ($\log g = 1.5$), and the highest metallicity of the sample ($[M/H] = 0.17$). We determined the minimal mass of the companion star to be at least $0.28 M_\odot$. The high rotational velocity indicates that the inclination could be close to $i = 90°$ suggesting that the secondary star is probably an M dwarf.

5.4 | HD 98812

The star HD 98812 is the most evolved star with a low value for the surface gravity of about $\log g = 1.0$. It has also the lowest effective temperature, 4,200 K. The mass was determined to be $2.15 M_\odot$, and the star has an age of 1.16 Gyr. The orbit is close to circular, and it has the lowest semi-amplitude with $K = 9.56$ km s^{-1}. The minimum mass of the secondary is $M_2 \sin i = 0.39 M_\odot$. Since the rotational velocity is low, it could be that the inclination is also lower. Thus, the actual mass of the secondary can be somewhat higher, either an M dwarf or even a K main-sequence star.

5.5 | HD 150600

HD 150600 is the star with the most eccentric orbit with $e = 0.5995$. The orbital period is about 123.2 days with a semi-amplitude of $K = 13.17$ km s^{-1}. The argument of the

T A B L E 5 The mass function (f) of the five spectroscopic binary systems, which we used to determine the minimum mass of the secondary stars (M_2)

Star	f ($M_\odot$)	M_1 ($M_\odot$)	$M_2 \sin i$ ($M_\odot$)
HD 20656	0.21632 ± 0.00115	2.73 ± 0.08	1.25 ± 0.02
HD 27259	0.01930 ± 0.00033	1.05 ± 0.15	0.28 ± 0.03
HD 98812	0.01242 ± 0.00019	2.15 ± 0.2	0.39 ± 0.02
HD 150600	0.01494 ± 0.00032	1.70 ± 0.2	0.36 ± 0.03
HD 193082	0.00506 ± 0.00008	1.88 ± 0.28	0.26 ± 0.03

periapsis of the star's orbit is $\omega = 76.26°$. The metallicity is close to solar. The star has a mass of $1.7 M_\odot$, has left the main sequence with an age of about 2.1 Gyr. However, the star is the closest to the main sequence in the HRD with a value for the surface gravity of $\log g = 3.0$. The companion has a minimal mass of $0.36 M_\odot$. The rotational velocity is low so that the mass of the companion could actually be larger.

5.6 | HD 193082

The system has the shortest period of the five stars, $P = 50.4$ days. The orbit is circular, and the semi-amplitude is about $K = 9.9$ km s^{-1}. The binary system has a high radial velocity of -89.7 km s^{-1} moving toward us and is marked in SIMBAD as a high proper-motion star.

The determined effective temperature ($T_{\text{eff}} = 4500$ K) indicates that the star is a K giant star instead of the SIMBAD classification of spectral type G8. The metallicity is $[M/H] = -0.32$, lower than the one of the Sun, but the abundances show clear α-enhancement with a value of 0.17. This star has a large rotation velocity of $v \sin i = 17.7$ km s^{-1} indicating that the inclination i is probably close to 90°. The mass of the primary is $M_1 = 1.9 M_\odot$, and the system has an age of 1.7 Gyr. The minimum mass of the secondary was determined to be only $M = 0.26 M_\odot$. Thus, the secondary star is probably an M dwarf.

5.7 | Estimating the binary effect on the parallax measurement

As mentioned above the orbital movement of the primary may alter the measurement of the parallax. Since we now know all orbital and stellar parameters, we can estimate the resulting error. Using the determined masses ($m_1 + m_2 = m_{\text{total}}$) and the periods P together with Kepler's laws it is possible to calculate the semi-major axis of the primary a_1. Using the distances one can calculate this as an angular separation α_1 in the sky. We found that this angle α_1 for four stars (HD 27259, HD 98812, HD 150600, HD 193082) is less than 1 mas. For HD 20656 the angle

is 1.1 mas, which corresponds to a possible error of 27% in the parallax. This is the maximum possible effect that the orbit may have on the parallax measurement. However, we do not know the orbital orientation and the period is also significantly lower than 1 year so that the several Gaia measurements during the few years of the mission may have averaged out this effect. The actual error is probably significantly lower.

6 | CONCLUSIONS

In this work, we determined all stellar and orbital parameters of five bright spectroscopic binary stars. Using spectral analysis, we determined the effective temperatures, surface gravities, and metallicities of the five stars. Using the effective temperatures and the Gaia DR2 parallaxes, we were able to determine the masses and ages by comparison with stellar evolution tracks. The orbital parameters were determined with the toolkit RadVel. Finally, an estimation of the masses of the respective secondary stars is presented. We found that two of the primary stars are wrongly classified in the SIMBAD database.

There is a significant number of bright and still undetected spectroscopic binary stars in the sky. We have already found 19 of them and presented a complete study of the orbits of five of them that have periods of $P < 365$ days in this work. In future work, we will continue our observations with the TIGRE telescope and present the orbital and stellar parameters of the remaining spectroscopic binaries with longer periods.

REFERENCES

Blanco-Cuaresma, S. 2019, *MNRAS*, *486*, 2075.

Blanco-Cuaresma, S., Soubiran, C., Heiter, U., & Jofré, P. 2014, *A&A*, *569*, A111.

Borucki, W. J., Koch, D., Basri, G., et al. 2010, *Science*, *327*, 977.

Duchêne, G., & Kraus, A. 2013, *ARA&A*, *51*, 269.

Flower, P. J. 1996, *ApJ*, *469*, 355.

Foreman-Mackey, D., Hogg, D. W., Lang, D., & Goodman, J. 2013, *PASP*, *125*, 306.

Fulton, B. J., Petigura, E. A., Blunt, S., & Sinukoff, E. 2018, *PASP*, *130*, 044504.

Gaia Collaboration, Prusti, T., de Bruijne, J. H. J., et al. 2016, *A&A*, *595*, A1.

Gaia Collaboration, Brown, A. G. A., Vallenari, A., et al. 2018, *A&A*, *616*, A1.

Gilmore, G., Randich, S., Asplund, M., et al. 2012, *Messenger*, *147*, 25.

Gray, R. O., & Corbally, C. J. 1994, *AJ*, *107*, 742.

Grevesse, N., Asplund, M., & Sauval, A. J. 2007, *Space Sci. Rev.*, *130*, 105.

Gustafsson, B., Edvardsson, B., Eriksson, K., Jørgensen, U. G., Nordlund, Å., & Plez, B. 2008, *A&A*, *486*, 951.

Husser, T. O., Wende-von Berg, S., Dreizler, S., Homeier, D., Reiners, A., Barman, T., & Hauschildt, P. H. 2013, *A&A*, *553*, A6.

Katz, D., Sartoretti, P., Cropper, M., et al. 2019, *A&A*, *622*, A205.

Kirk, B., Conroy, K., Prša, A., et al. 2016, *AJ*, *151*, 68.

Mason, B. D., Wycoff, G. L., Hartkopf, W. I., Douglass, G. G., & Worley, C. E. 2018, VizieR Online Data Catalog, 1.

Mittag, M., Hempelmann, A., Fuhrmeister, B., Czesla, S., & Schmitt, J. H. M. M. 2018, *AN*, *339*, 53.

Ochsenbein, F., Bauer, P., & Marcout, J. 2000, *A&AS*, *143*, 23.

Pols, O. R., Tout, C. A., Schroder, K.-P., Eggleton, P. P., & Manners, J. 1997, *MNRAS*, *289*, 869.

Pols, O. R., Schröder, K.-P., Hurley, J. R., Tout, C. A., & Eggleton, P. P. 1998, *MNRAS*, *298*, 525.

Pourbaix, D., Tokovinin, A. A., Batten, A. H., et al. 2004, *A&A*, *424*, 727.

Raghavan, D., McAlister, H. A., Henry, T. J., et al. 2010, *ApJS*, *190*, 1.

Randich, S., Gilmore, G., & Gaia-ESO Consortium 2013, *Messenger*, *154*, 47.

Schmitt, J. H. M. M., Schröder, K.-P., Rauw, G., et al. 2014, *AN*, *335*, 787.

Schröder, K. -P., Mittag, M., Flor Torres, L. M., Jack, D., & Snellen, I. 2020a, *MNRAS*, submitted.

Schröder, K. P., Mittag, M., Jack, D., Rodríguez Jiménez, A., & Schmitt, J. H. M. M. 2020b, *MNRAS*, *492*, 1110.

Taylor, S. F., Harvin, J. A., & McAlister, H. A. 2003, *PASP*, *115*, 609.

AUTHOR BIOGRAPHY

Dennis Jack is a full professor at the University of Guanajuato. He obtained his Diploma and PhD at the University of Hamburg. In 2012, he moved to Mexico and works on various topics in the field of stellar astrophysics.